*Journal of Sound and Vibration* (1999) **226**(3), 595–606
*Article No.* jsvi.1999.2267, available online at http://www.idealibrary.com on IDEAL®

# ANALYSES OF RELATIONSHIPS BETWEEN BIODYNAMIC RESPONSE FUNCTIONS

X. Wu, and S. Rakheja

*CONCAVE Research Center, Concordia University, 1455 boul. de Maisonneuve Ouest, Montreal, Quebec, Canada H3G 1M8*

AND

P.-É. Boileau

*Occupational Health and Safety Research Institute (IRSST), 505 boul. de Maisonneuve Ouest, Montreal, Quebec, Canada, H3A 3C2*

(*Received* 15 *March* 1999)

## 1. INTRODUCTION

The biodynamic response of the seated human body subjected to whole-body vibration can be characterized using three different biodynamic response functions. Two of these functions have often been used interchangeably to describe "to the body" force–motion relationship as a function of frequency at the human–seat interface, namely the driving-point mechanical impedance (DPMI) and the apparent mass (APMS). The DPMI relates the driving force and the resulting velocity response at the driving point, namely the seat-buttocks interface, and is given by

$$Z(\mathrm{j}\omega) = \frac{F(\mathrm{j}\omega)}{v(\mathrm{j}\omega)}, \tag{1}$$

where $Z(\mathrm{j}\omega)$ is the complex DPMI, and $F(\mathrm{j}\omega)$ and $v(\mathrm{j}\omega)$ are the driving force and response velocity at the driving point, respectively, $\omega$ is the angular frequency in rad/s. The APMS relates the driving force and the resulting acceleration response, and is related to the DPMI by

$$M(\mathrm{j}\omega) = \frac{F(\mathrm{j}\omega)}{a(\mathrm{j}\omega)} = \frac{Z(\mathrm{j}\omega)}{\mathrm{j}\omega}, \tag{2}$$

where $M(\mathrm{j}\omega)$ is the apparent mass and $a(\mathrm{j}\omega)$ is the driving point acceleration response. The magnitude of APMS has a simple physical interpretation that it is equal to the static mass of the human body supported by the seat at very low frequencies, when the human body effectively acts as a rigid mass. The acceleration

0022-460X/99/380595 + 12 $30.00/0 © 1999 Academic Press

response and the driving force thus remain in phase at low frequencies. The magnitude of DPMI can be obtained by multiplying the APMS by the angular frequency. The DPMI thus tends to emphasize the response at higher excitation frequencies, while the APMS yields more distinct peak response corresponding to primary resonant frequency. From the definitions of DPMI and APMS, it is apparent that DPMI leads the APMS by a constant 90° phase angle.

The third biodynamic response function constitutes a "through the body" biodynamic function, and is termed as a seat-to-head transmissibility (STHT), since it describes the vibration transmission through the body in the manner

$$H(\mathrm{j}\omega) = \frac{a_H(\mathrm{j}\omega)}{a(\mathrm{j}\omega)}, \tag{3}$$

where $H(\mathrm{j}\omega)$ is the complex seat-to-head transmissibility function and $a_H(\mathrm{j}\omega)$ is the head acceleration response. At low frequencies, the motion at the human–seat interface $a(\mathrm{j}\omega)$ is directly transmitted to the head due to the effectively rigid mass behavior of the human body, leading to a nearly unity value of transmissibility magnitude and relatively small phase difference.

The above three functions have been employed to characterize the human biodynamic response to vibration by performing measurements under a variety of test conditions, involving differences in subject masses, excitation levels, seated postures, etc. Researchers have used either DPMI or APMS to characterize "to the body" biodynamic response, depending upon their preferences or conveniences. For example, standardization efforts have concentrated on DPMI (ISO CD 5982 [1]), while Sandover [2] and Fairley and Griffin [3–5] have extensively reported the biodynamic response in terms of APMS functions. The benefits and limitations of using either function in presenting "to the body" biodynamic data, however, have not been addressed in the literature. It has generally been assumed that both functions described the force–motion relationships equivalently at the driving point. Some differences of significant importance, however, have been observed in the interpretation of the measured data, when presented in terms of the two functions. The most significant difference occurs in the estimation of the body's primary resonant frequency, which for either function, has been invariably taken as the frequency at which peak magnitude occurs [1–5]. As for the STHT which represents a "through the body" transfer function, its relationship with APMS appears to be more clear than that with the DPMI, although a theoretical link between these functions has never been attempted. A study of relationships between different forms of "to the body" biodynamic response functions, and "through the body" biodynamic functions may enhance the understanding of the biodynamic response behavior of the human body, and for defining a suitable model to represent the human body.

In this study, the relationships between the APMS, DPMI and STHT functions are investigated based upon both experimental data extracted from published studies and a theoretical analysis of four reported biodynamic models. On the basis of the results, recommendations are made as to the identification of the biodynamic response functions, which should be used for modelling purposes.

## 2. ANALYSES OF RELATIONSHIPS BETWEEN DPMI AND APMS FUNCTIONS

In an earlier study [6], an analysis of 14 published data sets, acquired under a similar range of test conditions, revealed extensive variations in the DPMI and APMS magnitudes, and the frequency at which peak magnitude is observed. Considering that this frequency represents the primary resonant frequency of the seated body, various APMS data sets revealed relatively less variations in the estimation of the primary resonant frequency, as opposed to DPMI for which the peak magnitude was found to vary between 4·0 to 7·0 Hz. The mean, standard deviation and range of the primary resonant frequency of the human body, estimated from these data sets are listed in Table 1, when the reported data are examined in terms of both DPMI and APMS.

From the results, it is apparent that analysis of data sets in terms of DPMI yields considerably larger variations in both standard deviation and range of estimated primary resonant frequency of the human body, when compared with those derived from the APMS function. The mean value of primary resonant frequency estimated from the DPMI data sets is higher than that from the APMS data sets. The same trend is also observed when the results obtained within a single study are considered, where a better control of the test conditions may be anticipated. The mean, standard deviation and range of the primary resonant frequency estimated from measured DPMI and APMS data of a group of seven subjects are summarized in Table 2. The data were measured under sinusoidal excitations swept in the 0·5–10 Hz frequency range, with acceleration of 1 $m/s^{-2}$ r.m.s. [7]. In this study, the subjects maintained an identical posture of upright upper body without back support with feet supported and vibrated. The results show trends similar to those observed in Table 1, although the standard deviation and range of primary

TABLE 1

*Variations in the primary resonant frequency of human body derived from the reported data sets in terms of DPMI and APMS*

| Function | Mean (Hz) | Standard deviation (Hz) | Range (Hz) |
|---|---|---|---|
| DPMI | 4·89 | 0·77 | 4·0–7·0 |
| APMS | 4·51 | 0·51 | 3·6–5·4 |

TABLE 2

*Variations in estimated primary resonant frequency of human body using data sets measured within a single study involving a group of seven subjects*

| Function | Mean (Hz) | Standard deviation (Hz) | Range (Hz) |
|---|---|---|---|
| DPMI | 4·84 | 0·22 | 4·5–5·4 |
| APMS | 4·75 | 0·17 | 4·5–5·0 |

resonant frequency of the subjects are seen to be considerably lower, which is most likely due to the identical test conditions pertaining to this data set. The variations, presented in Table 2, are therefore mainly attributed to the inter-subject variability.

The variations in the estimated whole-body resonant frequency from the DPMI and APMS functions are further investigated through analysis of four biodynamic models, reported in the literature and shown in Figure 1 [3, 8–10]. The equations of motion for the models considered, ranging from single- to two-degrees of freedom (d.o.f.), are solved to derive the expressions for modulus and phase of their respective DPMI and APMS. The resulting expressions are presented in Table 3, while parameters for the different model are summarized in Table 4. These expressions may be solved to determine the "to-the-body" biodynamic response in terms of DPMI or APMS and the primary resonant frequency, considered to correspond to the frequency at which the peak magnitudes occur.

The differences between the two functions may be related to their definition and the variations in the parameters of the models. A parameter sensitivity analysis is thus performed to study the variations in the primary resonant frequencies of the models with variations in the parameters, such as mass, stiffness and damping coefficients. The model parameters are varied by $\pm 20\%$ around the reported values, and the resulting APMS and DPMI magnitudes are analyzed to determine the sensitivity of the estimated primary resonant frequency ($f_p$) to variations in the model parameters. The primary resonant frequency corresponding to a specific

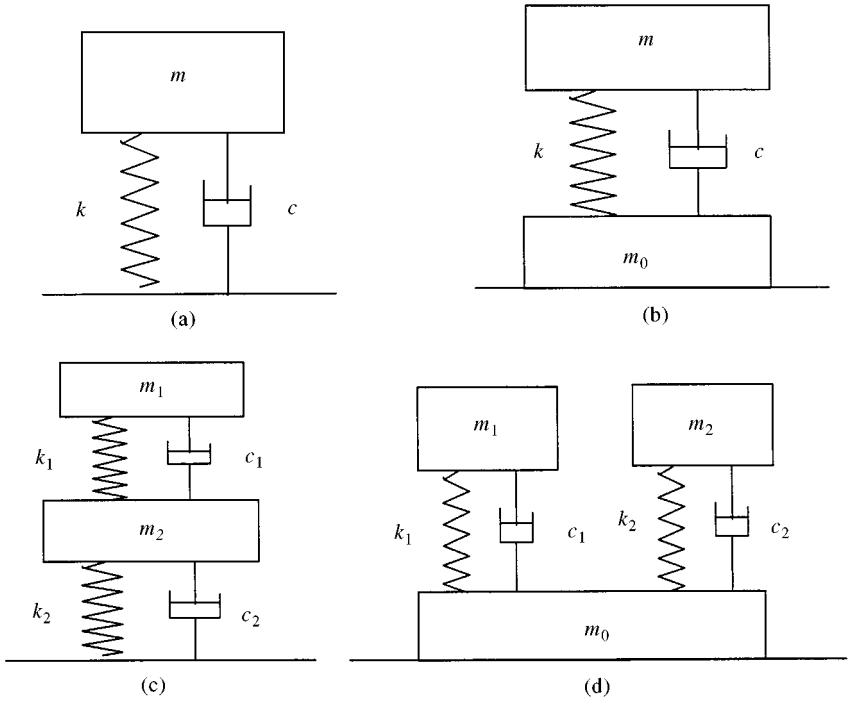


Figure 1. Selected biodynamic models: (a) Coermann [8], (b) Fairley and Griffin [3], (c) Allen [9], (d) Suggs *et al.* [10].

TABLE 3

*Expressions derived for the magnitude and phase of DPMI and APMS response functions of the selected models*

| Function | APMS | DPMI |
|---|---|---|
| Model | $M(\omega) = \sqrt{\frac{[A(\omega)]^2 + [B(\omega)]^2}{[C(\omega)]^2 + [D(\omega)]^2}}$<br>$\varphi(\omega) = a\tan\frac{B(w)}{A(w)} - a\tan\frac{D(w)}{C(\omega)}$ | $Z(\omega) = \omega M(\omega) = \omega\sqrt{\frac{[A(\omega)]^2 + [B(\omega)]^2}{[C(\omega)]^2 + [D(\omega)]^2}}$<br>$\varphi(\omega) = \frac{\pi}{2} + a\tan\frac{B(w)}{A(w)} - a\tan\frac{D(w)}{C(\omega)}$ |
| Coermann [8] | $A(\omega) = mk$<br>$B(\omega) = mc\omega$<br>$C(\omega) = k - m\omega^2$<br>$D(\omega) = c\omega$ | |
| Fairley and Griffin [3] | $A(\omega) = (m + m_0)k - m_0 m\omega^2$<br>$B(\omega) = (m + m_0)c\omega$<br>$C(\omega) = k - m\omega^2$<br>$D(\omega) = c\omega$ | |
| Allen [9] | $A(\omega) = (m_1 + m_2)k_1k_2 - (m_1c_1c_2 + m_2c_1c_2 + m_1m_2k_2)\omega^2$<br>$B(\omega) = (m_1 + m_2)(c_1k_2 + c_2k_1)\omega - m_1m_2c_2\omega^3$<br>$C(\omega) = k_1k_2 - (m_1k_2 + m_2k_1 + m_1k_1 + c_1c_2)\omega^2 + m_1m_2\omega^4$<br>$D(\omega) = (c_1k_2 + c_2k_1)\omega - (m_1c_2 + m_2c_1 + m_1c_1)\omega^3$ | |
| Suggs *et al.* [10] | $A(\omega) = (m + m_1 + m_2)k_1k_2 + mm_1m_2\omega^4 - [(m + m_1 + m_2)c_1c_2 + m(m_1k_2 + m_2k_1) + m_1m_2(k_1 + k_2)]\omega^2$<br>$B(\omega) = (m + m_1 + m_2)(k_1c_2 + k_2c_1)\omega - [m(m_1c_2 + m_2c_1) + m_1m_2(c_1 + c_2)]\omega^3$<br>$C(\omega) = k_1k_2 - (m_1k_2 + m_2k_1 + c_1c_2)\omega^2 + m_1m_2\omega^4$<br>$D(\omega) = (c_1k_2 + c_2k_1)\omega - (m_1c_2 + m_2c_1)\omega^3$ | |

TABLE 4

*Parameters of the selected models*

| Name of Model | Nominal model parameters |
|---|---|
| Coermann [8] | $f_n = 6{\cdot}3$ Hz, $k = 131181$ N/m, $\zeta = 0{\cdot}57$, $m = 83{\cdot}72$ kg |
| Fairley and Griffin [3] | $m = 45{\cdot}6$ kg, $m_0 = 6$ kg, $\zeta = 0{\cdot}475$, $c = 1360$ Ns/m, $f_n = 5$ Hz |
| Allen [9] | $m_1 = 5{\cdot}0$ kg, $\zeta_1 = 0{\cdot}05$, $f_{n1} = 17{\cdot}0$ Hz, $m_2 = 50{\cdot}0$ kg, $\zeta_2 = 0{\cdot}3$, $f_{n2} = 5{\cdot}0$ Hz |
| Suggs *et al.* [10] | $m_0 = 6$ kg, $m_1 = 36{\cdot}4$ kg, $m_2 = 18{\cdot}6$ kg, $k_1 = 25968$ N/m, $k_2 = 41549$ N/m, $c_1 = 485$ Ns/m, $c_2 = 884$ Ns/m |

functions is derived with an increase or decrease of 20% in a single parameter, while all the other parameters are held at their reported nominal values, as listed in Table 4. In this table, $f_n$ describes the undamped natural frequency of single-d.o.f. models proposed by Coermann [8], and Fairley and Griffin [3]. $f_{n1}$ and $f_{n2}$ are the two natural frequencies of the two-d.o.f. model proposed by Allen [9]. The mass, stiffness and damping parameters are represented by $(m, m_1, m_2)$ $(k, k_1, k_2)$, and $(c, c_1, c_2)$, respectively, as indicated in Figure 1. The damping ratio of the single-d.o.f. models [3, 8] is represented by $\zeta$, while $\zeta_1 = c_1/(2m_1\omega_{n1})$ and $\zeta_2 = c_2/(2m_2\omega_{n2})$ describe the uncoupled damping ratios of the two-d.o.f. model, proposed by Allen [9].

For models with more than one parameter of the same type, all the similar parameters are varied by the same amount ($\pm 20\%$) for each computation. For example, a $+20\%$ mass variation in the model proposed by Suggs *et al.* [10] is represented by an increase of 20% in all the three masses, and the corresponding primary resonant frequency is expressed as $f_{(m+20\%)}$. While the primary resonant frequency of the nominal model is represented by $f_p$, the sensitivity of the resonant frequency to variations in the model parameters is derived upon considering $\pm 20\%$ variations in all the model parameters. The sensitivity of the primary resonant frequency, $\Delta f_p$, is defined as the square root of the sum of squares of its variations due to change in each parameter or type of parameter:

$$\Delta f_p = [(f_p - f_{m-20\%})^2 + (f_p - f_{m+20\%})^2 + (f_p - f_{k-20\%})^2 + (f_p - f_{k+20\%})^2 + (f_p - f_{c-20\%})^2 + (f_p - f_{c+20\%})^2]^{1/2}. \quad (5)$$

The primary resonant frequency $f_p$ derived for each model with nominal parameters together with its sensitivities to variations in different parameters are presented in Table 5. The results show that the primary resonant frequency $f_p$ computed from

TABLE 5

*Sensitivity of the primary resonant frequencies, derived from DPMI and APMS magnitudes, to variations in model parameters*

| MODEL Function | Coermann [8] | | Fairley and Griffin [3] | | Allen [9] | | Suggs *et al.* [10] | |
|---|---|---|---|---|---|---|---|---|
| | DPMI | APMS | DPMI | APMS | DPMI | APMS | DPMI | APMS |
| $f_p$ (Hz) (nominal parameters) | 8·2 | 5·2 | 5·6 | 4·2 | 4·9 | 4·5 | 4·2 | 3·9 |
| $f_{m-20\%}$ (Hz) | 10·6 | 5·7 | 6·7 | 4·6 | 5·6 | 5·0 | 4·7 | 4·3 |
| $f_{m+20\%}$ (Hz) | 6·9 | 4·9 | 5·0 | 4·0 | 4·5 | 4·2 | 3·8 | 3·6 |
| $f_{k-20\%}$ (Hz) | 8·6 | 4·6 | 5·4 | 3·7 | 4·5 | 4·0 | 3·8 | 3·4 |
| $f_{k+20\%}$ (Hz) | 8·3 | 5·9 | 5·9 | 4·8 | 5·3 | 5·0 | 4·6 | 4·3 |
| $f_{c-20\%}$ (Hz) | 7·1 | 5·5 | 5·2 | 4·4 | 4·8 | 4·6 | 4·2 | 4·0 |
| $f_{c+20\%}$ (Hz) | 11·3 | 5·0 | 6·4 | 4·1 | 5·0 | 4·4 | 4·3 | 3·8 |
| $\Delta f_p$ (Hz) | 4·4 | 1·1 | 1·6 | 0·9 | 1·0 | 0·9 | 0·9 | 0·8 |

DPMI is consistently higher than that derived from APMS for all the four models. The $f_p$ derived from both the DPMI and APMS functions tends to decrease with an increase in mass parameters and increase with increase in the stiffness parameters. The variations in the damping coefficient(s), however, yield somewhat opposite trends in the primary resonant frequencies derived from DPMI and APMS magnitudes. An increase in the damping coefficient(s) yield higher primary resonant frequency estimated from the DPMI, and lower when derived from the APMS magnitude.

The results further show that the overall sensitivity of the primary resonant frequency, $\Delta f_p$, derived from DPMI magnitude, is larger than that derived from the APMS magnitude. The difference in the sensitivities derived on the basis of DPMI and APMS is specifically significant for single-d.o.f. models. The results further support the previous observations made from the measured and reported data that $\Delta f_p$ and $f_p$ derived from the APMS function tend to be smaller than those derived from the DPMI function. It can be thus concluded that the biodynamic measure of DPMI would most likely exhibit wider variations in the primary resonant frequency. Since the primary resonant frequency is of greatest interest in the study of human biodynamic response to vibration, the analyses of measured data in terms of APMS may lead to relatively smaller variations amongst the reported data sets. The "to the body" biodynamic response function in terms of APMS may thus be considered more appropriate for the purposes of synthesis of reported data and model development.

Furthermore, the "to the body" biodynamic response in terms of APMS can be derived from direct measurements of the driving-point force and the interface acceleration, while the computation of DPMI function involves digital integration of the measured acceleration signals. The derivation of APMS from the measured data requires only minimal effort for mass cancellation, when compared to that required for the DPMI.

## 3. ANALYSES OF RELATIONSHIP BETWEEN APMS AND STHT FUNCTIONS

Although not related by definition, some similarities have been observed between APMS and STHT response data [11, 12]. The measured magnitudes of AMPS and STHT tend to be constant at very low frequencies, and gradually approach their peak values at a similar frequency, followed by a gradual decrease as the excitation frequency increases. Although the four reported models were derived solely on the basis of DPMI or APMS function, it may be of interest to apply these models to explore analytically the possible relationship between STHT and APMS functions. The equations of motion, formulated for the four models, shown in Figure 1, are further analyzed to derived expressions for the normalized APMS and STHT magnitude and phase functions. Table 6 summarizes the expressions derived for normalized APMS and STHT functions for the four different models considered in the study. The normalization of APMS was realized upon dividing the APMS magnitude by the total mass of the model. Although the models do not describe a direct biomechanical representation of the head, the response of the mass at the extremity is taken to describe the motion of the head (mass $m$ in the single-d.o.f. models, and mass $m_1$ in the two-d.o.f. models).

The frequency response characteristics of both the normalized APMS and STHT for the selected models are illustrated in Figure 2. The magnitude and phase characteristics of both the functions for the single-d.o.f. model, proposed by Coremann [8], are identical, as expected from the expression appearing in Table 6. The single-d.o.f. model proposed by Fairley and Griffin [3] also yields almost identical results in the normalized APMS and STHT magnitudes over the entire frequency range, with identical phase response only up to 5 Hz. Since the normalized APMS function tends to suppress the magnitude of APMS at higher frequencies, the magnitude corresponding to the second resonance frequency of higher order models, in general, tends to be considerably lower. The model proposed by Allen [9] yields similar magnitudes of normalized APMS and STHT only at frequencies below 6 Hz, while the STHT magnitude response exhibits a significant second resonance at 17·7 Hz. It should be noted that APMS relates to the force–motion ratio divided by the square of the frequency. The APMS thus diminishes at higher frequencies. At excitation frequencies below 12 Hz, the phase response of the normalized APMS is almost identical to that of the STHT. The results derived from the model, proposed by Suggs *et al.* [10] yield a relatively large difference between the magnitudes of the normalized APMS and STHT in the vicinity of the primary resonant frequency, while both functions exhibit identical frequencies corresponding to peak magnitudes. At higher frequencies, however, both functions approach similar values in magnitude. The corresponding phase response of the two functions around the primary resonance is found to be quite similar.

Although certain differences between the magnitude and phase characteristics of the normalized APMS and STHT of the higher order models appear to exist, the primary resonant frequencies derived from these two functions are in very good agreement for all the models. The primary resonant frequencies derived from the STHT, APMS and DPMI functions for all four models investigated are

TABLE 6

*Expressions for the magnitude and phase of the normalized APMS and STHT of the selected models*

| | Normalized APMS | | STHT | |
|---|---|---|---|---|
| Model | $\text{Normalized } M(\omega) = \sqrt{\frac{[A(\omega)]^2 + [B(\omega)]^2}{[C(\omega)]^2 + [D(\omega)]^2}}$ | | $H(\omega) = \sqrt{\frac{[A(\omega)]^2 + [B(\omega)]^2}{[C(\omega)]^2 + [D(\omega)]^2}}$ | |
| | $\varphi(\omega) = \tan^{-1}\left[\frac{B(\omega)}{A(\omega)}\right] - \tan^{-1}\left[\frac{D(\omega)}{C(\omega)}\right]$ | | $\varphi(\omega) = \tan^{-1}\left[\frac{B(\omega)}{A(\omega)}\right] - \tan^{-1}\left[\frac{D(\omega)}{C(\omega)}\right]$ | |
| Coermann [8] | $A(\omega) = k,$ | $B(\omega) = c\omega$ | $A(\omega) = k,$ | $B(\omega) = c\omega$ |
| | $C(\omega) = k - m\omega^2,$ | $D(\omega) = c\omega$ | $C(\omega) = k - m\omega^2,$ | $D(\omega) = c\omega$ |
| Fairley and Griffin [3] | $A(\omega) = k - \frac{m_0 m}{m_0 + m}\omega^2,$ | $B(\omega) = c\omega$ | $A(\omega) = k,$ | $B(\omega) = c\omega$ |
| | $C(\omega) = k - m\omega^2,$ | $D(\omega) = c\omega$ | $C(\omega) = k - m\omega^2,$ | $D(\omega) = c\omega$ |
| Allen [9] | $A(\omega) = k_1 k_2 - \left(c_1 c_2 + \frac{m_1 m_2}{m_1 + m_2} k_2\right)\omega^2$ | | $A(\omega) = k_1 k_2 - c_1 c_2 \omega^2,$ | |
| | $B(\omega) = (c_1 k_2 + c_2 k_1)\omega - \frac{m_1 m_2}{m_1 + m_2} c_2 \omega^3$ | | $B(\omega) = (c_1 k_2 + c_2 k_1)\omega,$ | |
| | $C(\omega) = k_1 k_2 - (m_1 k_2 + m_2 k_1 + m_1 k_1 + c_1 c_2)\omega^2 + m_1 m_2 \omega^4$ | | $C(\omega) = k_1 k_2 - (m_1 k_2 + m_2 k_1 + m_1 k_1 + c_1 c_2)\omega^2 + m_1 m_2 \omega^4$ | |
| | $D(\omega) = (c_1 k_2 + c_2 k_1)\omega - (m_1 c_2 + m_2 c_1 + m_1 c_1)\omega^3$ | | $D(\omega) = (c_1 k_2 + c_2 k_1)\omega - (m_1 c_2 + m_2 c_1 + m_1 c_1)\omega^3$ | |
| | $A(\omega) = k_1 - \left[\frac{c_1 c_2}{k_2} + \frac{(m + m_1)m_2}{m + m_1 + m_2}\frac{k_1}{k_2} + \frac{(m + m_2)m_1}{m + m_1 + m_2}\right]\omega^2 + \frac{m m_1 m_2}{m + m_1 + m_2}\frac{1}{k_2}\omega^4$ | | $A(\omega) = k_1$ | |
| Suggs *et al.* [10] | $B(\omega) = \left(c_1 + c_2\frac{k_1}{k_2}\right)\omega - \left[\frac{(m + m_1)m_2}{m + m_1 + m_2}\frac{c_1}{k_2} + \frac{(m + m_2)m_1}{m + m_1 + m_2}\frac{c_2}{k_2}\right]\omega^3$ | | $B(\omega) = c_1\,\omega$ | |
| | $C(\omega) = k_1 - \left(m_1 + m_2\frac{k_1}{k_2} + \frac{c_1 c_2}{k_2}\right)\omega^2 + \frac{m_1 m_2}{k_2}\omega^4$ | | $C(\omega) = k_1 - m_1\omega^2$ | |
| | $D(\omega) = \left(c_1 + c_2\frac{k_1}{k_2}\right)\omega - \left(\frac{m_1 c_2 + m_2 c_1}{k_2}\right)\omega^3$ | | $D(\omega) = c_1\,\omega$ | |

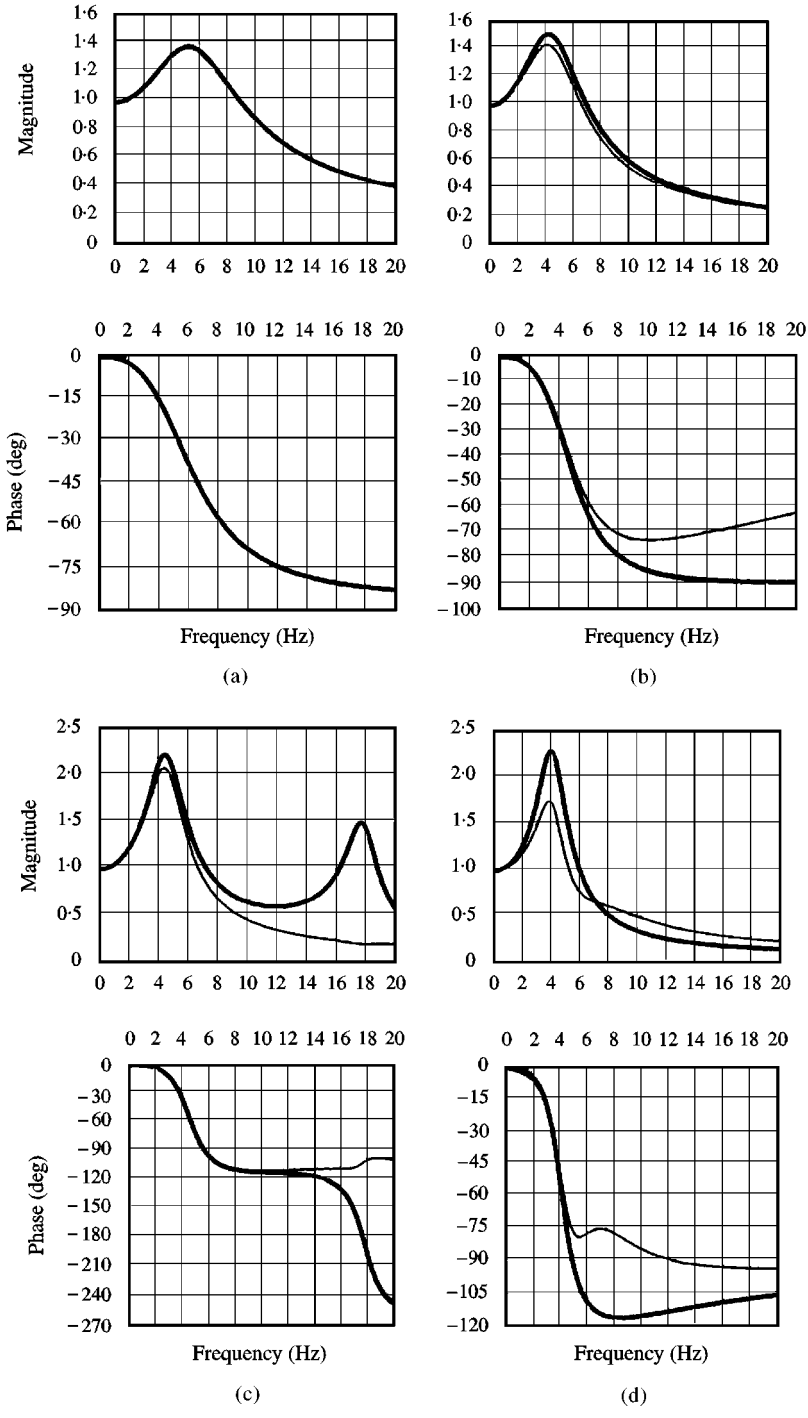


Figure 2. Magnitudes and phases of both normalized APMS and STHT for the four biodynamic models: (a) Coermann [8], (b) Fairley and Griffin [3], (c) Allen [9], (d) Suggs *et al.* [10]; ▬, normalized APMS; ▬, STHT.

TABLE 7

*Comparison of primary resonant frequencies of the selected models derived from different functions*

| Model | Primary resonant frequency (Hz) | | | |
|---|---|---|---|---|
| | Coermann [8] | Fairley and Griffin [3] | Allen [9] | Suggs *et al.* [10] |
| Eigenvalue analysis | 5·2 | 4·4 | 4·6 | 4·1 |
| STHT magnitude | 5·2 | 4·3 | 4·5 | 4·0 |
| APMS magnitude | 5·2 | 4·2 | 4·5 | 3·9 |
| UPMI magnitude | 8·2 | 5·6 | 4·9 | 4·2 |

summarized in Table 7 using the nominal model parameter values presented in Table 4. An eigenvalue analysis of the selected models was further performed to identify their primary damped resonant frequencies. For all the four models, the STHT and APMS functions yield almost identical primary resonant frequencies, which are considerably different from those derived from the DPMI function, except perhaps for the model developed by Suggs *et al.* [10]. The reported studies have invariably identified the primary resonant frequencies from the peak magnitudes of the biodynamic response function considered. The results clearly show that the resonant frequencies estimated from the different functions may differ considerably. The results of an eigenvalue analysis, also listed in Table 7, show that the primary resonant frequencies predicted from STHT and APMS functions are in better agreement with those computed from an eigenvalue analysis. The APMS and STHT functions are thus considered to represent the primary resonant frequency of the body more accurately, which should not vary with the use of a different biodynamic function since it represents inherent body characteristics. In contrast, the primary resonant frequencies, predicted from DPMI, tend to differ considerably from those derived from the eigenvalue analysis, depending upon the model considered. These results suggest that if a model is to be based on both "to the body" and 'through the body" functions, the APMS and STHT functions should be selected. Attempts to use DPMI along with STHT would result in wide discrepancies in the estimated response and the primary resonant frequency. Furthermore, the results also suggest that it should be possible to develop a seated body model with relatively fewer d.o.f., on the basis of analytical functions and measured data.

## 4. CONCLUSIONS

The relationships between different measures of "to the body" biodynamic response functions, and between "to" and "through" the body biodynamic functions are investigated based on both experimental data and analysis of some of the reported seated body models. From the analysis of measured data, derived from

either different studies or from different subjects considered in a single study, it is concluded that the analysis based upon APMS magnitude yields considerably less variations in the primary resonant frequency identified from different data sets. The analyses of the measured data and four different analytical models further revealed relatively larger variations in the primary resonant frequency derived from the DPMI magnitude, when compared to that attained from the APMS. A close agreement between the normalized APMS and STHT functions is also established in terms of the magnitudes and the primary resonant frequency of the seated body. The primary resonant frequencies estimated from the normalized APMS and STHT further showed excellent agreement with those derived from eigenvalue analysis of the models. It is thus concluded that the APMS and STHT data are more likely to reveal the inherent damped resonant frequency of the body than the DPMI. APMS and STHT functions thus appear to represent the most appropriate transfer functions for model development based on both "to the body" and and "through the body" response characteristics.

## REFERENCES

1. *International Standard for Standardization* 1993 *Draft CD* 5982. Mechanical driving point impedance and transmissibility of the human body.
2. J. Sandover 1982, *Ph.D. Thesis*, *Loughborough University of Technology*. Measurements of the frequency response characteristics of man exposed to vibration.
3. T. E. Fairley and M. J. Griffin 1989 *Journal of Biomechanics* **22**, 81–94. The apparent mass of the seated human body: vertical vibration.
4. T. E. Fairley and M. J. Griffin 1983 *International Conference on Noise Control Engineering*, Edinburgh, 533–536. Application of mechanical impedance methods to seat transmissibility.
5. T. E. Fairley and M. J. Griffin 1986 *Society of Automotive Engineer International Congress and Exposition*, *Detroit*, 24–28 *February*, *SAE* 860046. A test method for predicting of seat transmissibility.
6. P.-É. Boileau, X. Wu and S. Rakheja 1998 *Journal of Sound Vibration* **215**, 841–862. Definition of a range of idealized values to characterize seated body biodynamic response under vertical vibration.
7. P.-É. Boileau and S. Rakheja 1998 *International Journal of Industrial Ergonomics* **22**, 449–472. Whole-body vertical biodynamic response characteristics of the seated vehicle driver: measurement and model development.
8. R. R. Coermann 1962 *Human Factors*, 227–253. The mechanical impedance of the human body in sitting and standing position at low frequencies.
9. G. Allen 1978 Paper A25-5, *AGARD Conference Proceedings No*. 253, *Paris*, *France*, 6-10 *November*. A critical look at biodynamic modeling in relation to specifications for human tolerance of vibration and shock.
10. C. W. Suggs, C. F. Abrams and L. F. Stikeleather 1969 *Ergonomics*, **12**, 79–90. Application of a damped spring–mass human vibration simulator in vibration testing of vehicle seats.
11. X. Wu 1998 *Ph.D. Thesis*, Concordia University, Montreal, Canada. Study of driver-seat interactions and enhancement of vehicular ride vibration environment.
12. B. Hinz and H. Seidel 1987 *Industrial Health* **25**, 169–181. The nonlinearity of the human body's dynamic response during sinusoidal whole body vibration.